Two-state model for helicase translocation and unwinding of nucleic acids

Ashok Garai,[1,*] Debashish Chowdhury,[1,2,†] and M. D. Betterton[3,‡]

[1]*Department of Physics, Indian Institute of Technology, Kanpur 208016, India*
[2]*Max-Planck Institute for Physics of Complex Systems, Nöthnitzer Strasse 38, D-01187 Dresden, Germany*
[3]*Physics Department, University of Colorado, Boulder, Colorado 80309-0390, USA*

Helicases are molecular motors that unwind double-stranded nucleic acids (dsNA), such as DNA and RNA. Typically a helicase translocates along one of the NA single strands while unwinding and uses adenosine triphosphate (ATP) hydrolysis as an energy source. Here we model a helicase motor that can switch between two states, which could represent two different points in the ATP hydrolysis cycle. Our model is an extension of the earlier Betterton-Jülicher model of helicases to incorporate switching between two states. The main predictions of the model are the speed of unwinding of the dsNA and fluctuations around the average unwinding velocity. Motivated by a recent claim that the NS3 helicase of Hepatitis C virus follows a flashing-ratchet mechanism, we have compared the experimental results for the NS3 helicase with a special limit of our model which corresponds to the flashing-ratchet scenario. Our model accounts for one key feature of the experimental data on NS3 helicase. However, contradictory observations in experiments carried out under different conditions limit the ability to compare the model to experiments.

PACS number(s): 87.16.Nn, 82.39.−k, 87.10.−e, 87.15.A−

I. INTRODUCTION

Helicases are enzymes that unwind double-stranded nucleic acids (dsNA) [1]. Helicase proteins typically translocate along one of the single strands and perform mechanical work while consuming chemical energy [usually supplied by the hydrolysis of adenosine triphosphate (ATP)]. Therefore, these NA translocases are molecular motors [2,3] which share common features with cytoskeletal molecular motors [4,5].

All helicases undergo a biochemical cycle which typically involves ATP binding, ATP hydrolysis, and release of the hydrolysis products adenosine diphosphate (ADP) and inorganic phosphate (P_i). An important goal in the study of helicase mechanisms is to understand how the ATP hydrolysis cycle is coupled to the binding state and the motion of the helicase [6,7]. Helicases may exhibit changes in helicase-NA binding affinity when the helicase is bound to ATP, ADP/P_i, or neither; coordination of hydrolysis between different helicase subunits, and conformational changes in the helicase triggered by different steps in the hydrolysis cycle. Some helicases form hexamers (which include six ATPase domains), while others are members of the nonhexameric (dimeric or monomeric) group; different types of mechanochemical cycle have been suggested for the different structural classes [6,8]. In all cases, one seeks to explain how the helicase coordinates NA binding and hydrolysis to move along single-stranded NA and unwind double-stranded NA.

Here we develop a generic model of a helicase that switches between two biochemical states while translocating on ssNA. This is a simplified representation of the different states of the helicase during the ATP hydrolysis cycle. The model may be generally applicable to helicases for which the transition between two states is the key feature of the motion. In other words, this model should be a good approximation for helicases with more than two biochemical states if one transition is far slower than the others. We incorporate such a two-state picture by extending the original Betterton-Jülicher (BJ) model [9–11] of NA helicases [12].

Our work is also connected to two-state models that have been used extensively for a variety of molecular motors [13–16]. Under a mean-field approximation, such models can be easily solved when periodic boundary conditions are imposed. However, the problem is usually more difficult with open boundary conditions. The model for helicase motion is even more complex because the position of one boundary (i.e., the ssNA-dsNA junction) varies randomly with time. Thus our work is also an extension of previous work on two-state models to the more difficult case of a fluctuating boundary.

The two-state model developed here is consistent with the observation that binding and hydrolysis of ATP can modulate the affinity of a helicase for the nucleic-acid track [17–19]. The flashing-ratchet mechanism suggested qualitatively for the hepatitis C virus nonstructural protein 3 (HCV NS3) helicase [20,21] can be captured by a special case of the generic model proposed here. In the flashing-ratchet [13] picture, the motor protein switches between two states: one where the protein is tightly bound to the track and another where the motor is weakly bound and can diffuse along the track. In this paper we make quantitative comparisons between our theoretical predictions for a passive helicase which follows the flashing-ratchet mechanism and the experimental data for NS3 helicase.

In Sec. II we describe the ingredients of the model: the helicase, which can switch between two states and translocate on ssNA, and the fluctuating NA ss-ds junction. In Sec. III we calculate the single-strand translocation rate of the helicase. Section IV contains the model equations for double-strand unwinding, the transformation of the equations

---

*garai@iitk.ac.in
†debch@iitk.ac.in
‡mdb@colorado.edu

using midpoint and difference variables, and the general solutions for the velocity and diffusion coefficient. We describe the results for a hard-wall interaction between the helicase and junction in Sec. V. Using rate constants estimated from experiments on NS3 helicase, in Sec. VI we specialize to the flashing-ratchet scenario and make predictions specific to NS3. In Sec. VII we summarize our results.

II. MODEL

Here we develop a physical model for a helicase that moves on ssNA while cycling between two chemical states (labeled 1 and 2). Levin *et al.* suggested such a two-state model for NS3 helicase motion [20,21]. In this paper, we first consider a general two-state model and later focus on the specific flashing-ratchet picture.

In the traditional continuous models of Brownian ratchets, one first writes a Fokker-Planck equation. We use a discrete model, so our approach is based on master equations. The discrete approach can be useful when comparing to experiments. In the Fokker-Planck approach, one needs the explicit functional form of the fluctuating potential, which has not been measured for any real motor. In the discrete model, we bypass this difficulty by capturing the motor mechanism through a choice of rate constants (or transition probabilities), many of which can be obtained from experiments (see Sec. VI).

In the discrete model, we represent the ssNA by a one-dimensional lattice where each site corresponds to a single base. We label each site by the integer index i. As in the BJ model [9], we neglect the sequence inhomogeneity of the ssNA (in principle, the model can be extended to capture this feature, which may be important in some limits [22]). The position of the helicase is denoted by the integer n. Most helicases have a fixed direction of translocation, either 3′ to 5′ or 5′ to 3′ along the left-right asymmetric ssNA [6]. In our model the helicase translocates toward increasing n (from left to right in Fig. 1). At any spatial position n, the helicase can be either in biochemical state 1 or 2.

The model is fully described by the allowed transitions between states and the corresponding reaction rates. In general, we could have all transitions sketched in Fig. 1. Helicase "sliding" corresponds to transitions along the ssNA without a change in biochemical state of the protein. In state 1, these sliding transitions occur at rate s_{1f} (for increasing n) and s_{1b} (for decreasing n). When the helicase is in state 2, the forward and backward sliding rates are s_{2f} and s_{2b}. Physically, these transitions occur because of Brownian motion of the protein, decoupled from any biochemical state change.

The helicase can undergo "chemical" transitions which correspond to a change in biochemical state without physical translocation along the ssNA. At fixed n, the rate of transition from state 1 to 2 occurs at rate ω_{12}, while the reverse transition occurs at rate ω_{21}. Finally, "coupled" mechanochemical transitions are those where a change of biochemical state and physical translocation occur together. If the helicase is located at n and is in state 2, then it can make a transition to state 1 while moving forward to site $n+1$ at rate r_f; the corresponding reverse rate is r_b. The transition of
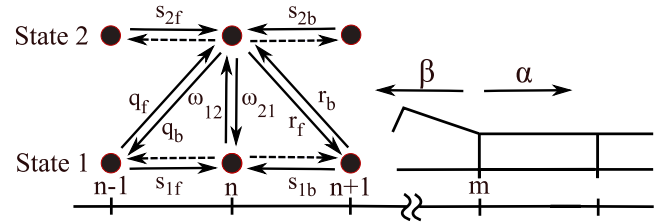

FIG. 1. (Color online) Schematic of the model. The protein can exist in either of two chemical states (labeled 1 and 2) at each lattice site (labeled n). Sliding transitions (where n changes, but the chemical state does not) occur at rate s_{1f}, etc., depending on the state and whether the transition is forward (toward increasing n) or backward (toward decreasing n). Chemical transitions (where the chemical state changes, but n does not) occur at rates ω_{12} (for the transition from 1 to 2) and ω_{21} (for the transition from 2 to 1). Coupled transitions, where both the chemical state and n change, occur at rates r_f (for the transition from 2 to 1 coupled to forward motion), r_b (for the transition from 1 to 2 coupled to backward motion), q_f (for the transition from 1 to 2 coupled to forward motion), and q_b (for the transition from 2 to 1 coupled to backward motion). The nucleic-acid single-strand–double-strand junction is at site m. The junction moves toward increasing m when the NA opens by one base (rate α) and toward decreasing m when the NA closes (rate β).

the helicase from state 1 to 2 while moving forward from n to $n+1$ occurs at rate q_f; the corresponding reverse rate is q_b.

If any of these reactions is coupled to ATP hydrolysis, then the forward and reverse transitions may be out of equilibrium and break the detailed balance relation. The model of Levin *et al.* of HCV NS3 helicase suggests that ATP binding is required to remove the helicase from the tightly bound state [20,21], implying that the $1 \to 2$ transition at rate ω_{12} is determined by the ATP concentration. In the flashing-ratchet model of Levin *et al.*, ATP hydrolysis and product release are coupled to the translocation and chemical transition back to state 1, which in our representation means that rates ω_{21} and r_f would be coupled to ATP hydrolysis and would therefore be out of equilibrium (see Sec. VI).

The junction between ssNA and dsNA is labeled by m (see Fig. 1). The dsNA opens and closes due to thermal fluctuations. When the helicase and junction are far apart, the opening rate is α and the closing rate β. We assume that these rates are independent of the NA base sequence and that the only fluctuations are those for which the NA opens or closes at the ss-ds fork. Following the BJ model [9], we neglect the possibility of any jump >1 bp in the position of the ssNA-dsNA junction. However, this approximation is justified because, at the temperatures of our interest (i.e., sufficiently below the melting temperature of the dsDNA), the spontaneous formation of bubbles is rare. Since the NA breathing results from thermal fluctuations, the rates α and β satisfy detailed balance: $\frac{\alpha}{\beta} = e^{-\Delta G}$, where ΔG is the free energy of one base-pair bond in units of kT.

The main quantity of interest is the speed of unwinding of dsNA by a helicase. We derive an analytical expression for the unwinding velocity. We compare the predicted velocity with the corresponding experimental data for a specific helicase: NS3 helicase of hepatitis C virus. Although we also

derive an analytical expression for the diffusion constant of the helicase, we do not compare it with experimental data for any specific helicase.

In this work we analyze passive unwinding, which is equivalent to a hard-wall interaction potential in the BJ model [10]. In passive unwinding, the helicase acts as a block to NA closing when adjacent to the junction. The protein moves forward only when thermal fluctuations open a base pair at the NA ss-ds junction. This means that when the helicase and junction are adjacent ($j=1$), the helicase cannot hop forward [all helicase forward rates $s_{1f}(j=1)$, $s_{2f}(j=1)$, $r_f(j=1)$, and $q_f(j=1)$ are zero] and the NA cannot close [$\beta(j=1)=0$]. Otherwise, the rates are unaffected by the helicase-junction interaction.

III. SINGLE-STRAND TRANSLOCATION

In order to motivate our approach, we first formulate the equations for a helicase sufficiently far from the ssNA-dsNA junction so that it translocates on ssNA without any dsNA unwinding activity. Let $\mathcal{P}_\mu(n,t)$ denote the probability that, at time t, the helicase is located at site n and is in the chemical state μ. We will drop the reference to the time dependence of $\mathcal{P}_\mu(n)$. The master equations governing the time evolution of $\mathcal{P}_\mu(n)$ are

$$\frac{d\mathcal{P}_1(n)}{dt} = -(\omega_{12} + s_{1f} + s_{1b} + q_f + r_b)\mathcal{P}_1(n)$$
$$+ s_{1f}\mathcal{P}_1(n-1) + r_f\mathcal{P}_2(n-1) + s_{1b}\mathcal{P}_1(n+1)$$
$$+ q_b\mathcal{P}_2(n+1) + \omega_{21}\mathcal{P}_2(n) \quad (1)$$

and

$$\frac{d\mathcal{P}_2(n)}{dt} = -(\omega_{21} + s_{2f} + s_{2b} + r_f + q_b)\mathcal{P}_2(n) + s_{2f}\mathcal{P}_2(n-1)$$
$$+ q_f\mathcal{P}_1(n-1) + s_{2b}\mathcal{P}_2(n+1) + r_b\mathcal{P}_1(n+1)$$
$$+ \omega_{12}\mathcal{P}_1(n). \quad (2)$$

Summing these equations, we find that the total probability $\mathcal{P}(n) = \mathcal{P}_1(n) + \mathcal{P}_2(n)$ satisfies

$$\frac{d\mathcal{P}(n)}{dt} = -(s_{1f} + s_{1b} + q_f + r_b)\mathcal{P}_1(n)$$
$$- (s_{2f} + s_{2b} + r_f + q_b)\mathcal{P}_2(n) + (s_{1f} + q_f)\mathcal{P}_1(n-1)$$
$$+ (s_{2f} + r_f)\mathcal{P}_2(n-1) + (s_{1b} + r_b)\mathcal{P}_1(n+1)$$
$$+ (s_{2b} + q_b)\mathcal{P}_2(n+1). \quad (3)$$

These equations have a translationally invariant steady-state solution where $\mathcal{P}_\mu(n)$ is independent of n. In this case, we expect that the probability in state 2 is a multiple of the probability in state 1:

$$\mathcal{P}_2(n) = \sigma\mathcal{P}_1(n), \quad (4)$$

which means that $\mathcal{P}(n) = (1+\sigma)\mathcal{P}_1(n)$.

In this case, the master equation for the total probability can be written as a hopping model with effective rates k_f for

forward transitions and k_b for backward transitions. At steady state,

$$0 = k_f\mathcal{P}(n-1) - (k_f + k_b)\mathcal{P}(n) + k_b\mathcal{P}(n+1), \quad (5)$$

where

$$k_f = \frac{s_{1f} + q_f + \sigma(s_{2f} + r_f)}{1+\sigma}, \quad (6)$$

$$k_b = \frac{s_{1b} + r_b + \sigma(s_{2b} + q_b)}{1+\sigma}, \quad (7)$$

and the expression

$$\sigma = \frac{\omega_{12} + q_f + r_b}{r_f + q_b + \omega_{21}} \quad (8)$$

has been obtained from Eq. (1) at steady state, assuming translational invariance. The mean single-strand translocation velocity is $v_{ss} = k_f - k_b$.

IV. DOUBLE-STRAND UNWINDING: MODEL EQUATIONS

In this section we extend the formulation of the preceding section by incorporating helicase-catalyzed dsNA unwinding. Let $\mathcal{P}_\mu(n,m;t)$ denote the probability that, at time t, the helicase is located at n and is in the chemical state μ, while the ss-ds junction is at m. We will drop the reference to the time dependence of $\mathcal{P}_\mu(n,m)$. The master equations governing the time evolution of $\mathcal{P}_\mu(n,m)$ are given by

$$\frac{d\mathcal{P}_1(n,m)}{dt} = -(\alpha + \beta + \omega_{12} + s_{1f} + s_{1b} + q_f + r_b)\mathcal{P}_1(n,m)$$
$$+ s_{1f}\mathcal{P}_1(n-1,m) + r_f\mathcal{P}_2(n-1,m)$$
$$+ s_{1b}\mathcal{P}_1(n+1,m) + q_b\mathcal{P}_2(n+1,m) + \omega_{21}\mathcal{P}_2(n,m)$$
$$+ \alpha\mathcal{P}_1(n,m-1) + \beta\mathcal{P}_1(n,m+1) \quad (m > n) \quad (9)$$

and

$$\frac{d\mathcal{P}_2(n,m)}{dt} = -(\alpha + \beta + \omega_{21} + s_{2f} + s_{2b} + r_f + q_b)\mathcal{P}_2(n,m)$$
$$+ s_{2f}\mathcal{P}_2(n-1,m) + q_f\mathcal{P}_1(n-1,m)$$
$$+ s_{2b}\mathcal{P}_2(n+1,m) + r_b\mathcal{P}_1(n+1,m) + \omega_{12}\mathcal{P}_1(n,m)$$
$$+ \alpha\mathcal{P}_2(n,m-1) + \beta\mathcal{P}_2(n,m+1) \quad (m > n). \quad (10)$$

Note that the rates depend on the separation $m-n$; this notation is omitted for clarity. We assume that the interaction potential is the same for both chemical states, so that the position-dependent NA opening and closing rates α and β are independent of the chemical state.

Next we change variables to work with the difference $j = m - n$ and midpoint $l = 2l' = m + n$ positions of the helicase-junction complex. Rewriting Eqs. (9) and (10) we have

$$\frac{d\mathcal{P}_1(j,l)}{dt} = -(\alpha + \beta + \omega_{12} + s_{1f} + s_{1b} + q_f + r_b)\mathcal{P}_1(j,l)$$

$$+ s_{1f}\mathcal{P}_1(j+1,l-1) + r_f\mathcal{P}_2(j+1,l-1)$$

$$+ s_{1b}\mathcal{P}_1(j-1,l+1) + q_b\mathcal{P}_2(j-1,l+1)$$

$$+ \omega_{21}\mathcal{P}_2(j,l) + \alpha\mathcal{P}_1(j-1,l-1)$$

$$+ \beta\mathcal{P}_1(j+1,l+1) \quad (j > 0) \tag{11}$$

and

$$\frac{d\mathcal{P}_2(j,l)}{dt} = -(\alpha + \beta + \omega_{21} + s_{2f} + s_{2b} + r_f + q_b)\mathcal{P}_2(j,l)$$

$$+ s_{2f}\mathcal{P}_2(j+1,l-1) + q_f\mathcal{P}_1(j+1,l-1)$$

$$+ s_{2b}\mathcal{P}_2(j-1,l+1) + r_b\mathcal{P}_1(j-1,l+1)$$

$$+ \omega_{12}\mathcal{P}_1(j,l)$$

$$+ \alpha\mathcal{P}_2(j-1,l-1) + \beta\mathcal{P}_2(j+1,l+1) \quad (j > 0). \tag{12}$$

Again, the rates vary with j. However, the rates are independent of l, so we can sum over the position of the complex center of mass:

$$P_1(j) = \sum_l \mathcal{P}_1(j,l),$$

$$P_2(j) = \sum_l \mathcal{P}_2(j,l). \tag{13}$$

Applying the sum over l to Eqs. (11) and (12) we find

$$\frac{dP_1(j)}{dt} = -(\alpha + \beta + \omega_{12} + s_{1f} + s_{1b} + q_f + r_b)P_1(j) + (s_{1f}$$

$$+ \beta)P_1(j+1) + r_f P_2(j+1) + (s_{1b} + \alpha)P_1(j-1)$$

$$+ q_b P_2(j-1) + \omega_{21}P_2(j) \tag{14}$$

and

$$\frac{dP_2(j)}{dt} = -(\alpha + \beta + \omega_{21} + s_{2f} + s_{2b} + r_f + q_b)P_2(j)$$

$$+ (s_{2f} + \beta)P_2(j+1) + q_f P_1(j+1)$$

$$+ (s_{2b} + \alpha)P_2(j-1) + r_b P_1(j-1) + \omega_{12}P_1(j). \tag{15}$$

We consider the total probability by summing Eqs. (14) and (15). Defining the total probability current

$$I(j) = \alpha P(j) - \beta P(j+1) + (s_{1b} + r_b)P_1(j) + (s_{2b} + q_b)P_2(j)$$

$$- (s_{1f} + q_f)P_1(j+1) - (s_{2f} + r_f)P_2(j+1), \tag{16}$$

the total probability satisfies

$$\frac{dP(j)}{dt} = -I(j) + I(j-1). \tag{17}$$

At steady state $P(j)$ is time independent, so $I(j) = I(j-1)$. Further, since $U(j) \to \infty$ as $j \to -\infty$, this constant probability flux must be zero—i.e., $I(j) = 0$ for all j.

Adding the two equations (11) and (12) and defining $\mathcal{P}(j,l) = \mathcal{P}_1(j,l) + \mathcal{P}_2(j,l)$, we get

$$\frac{d\mathcal{P}(j,l)}{dt} = -(\alpha + \beta)\mathcal{P}(j,l) + \alpha\mathcal{P}(j-1,l-1)$$

$$+ \beta P(j+1,l+1) + (s_{1f} + q_f)\mathcal{P}_1(j+1,l-1)$$

$$+ (r_f + s_{2f})\mathcal{P}_2(j+1,l-1)$$

$$+ (s_{1b} + r_b)\mathcal{P}_1(j-1,l+1)$$

$$+ (q_b + s_{2b})\mathcal{P}_2(j-1,l+1) + \omega_{21}\mathcal{P}_2(j,l)$$

$$+ \omega_{12}\mathcal{P}_1(j,l) - (\omega_{12} + s_{1f} + s_{1b} + q_f + r_b)\mathcal{P}_1(j,l)$$

$$- (\omega_{21} + s_{2f} + s_{2b} + r_f + q_b)\mathcal{P}_2(j,l). \tag{18}$$

The probability distribution in l at time t is

$$\Pi(l;t) = \sum_j \mathcal{P}(j,l;t). \tag{19}$$

Note that, by definition, $\Pi(l;t)$ is independent of the chemical state of the helicase. For times much longer than the relaxation time of the difference variable j, we can assume

$$\mathcal{P}_\mu(j,l) = P_\mu(j)\Pi(l) \quad (\mu = 1 \text{ or } 2). \tag{20}$$

Starting from Eq. (18), one can derive

$$\frac{d\Pi(l)}{dt} = u\Pi(l-1) - (u+w)\Pi(l) + w\Pi(l+1), \tag{21}$$

where

$$u = \sum_j \alpha P(j) + (s_{1f} + q_f)P_1(j) + (s_{2f} + r_f)P_2(j) \tag{22}$$

and

$$w = \sum_j \beta P(j) + (s_{1b} + r_b)P_1(j) + (s_{2b} + q_b)P_2(j). \tag{23}$$

Thus the motion of the helicase-junction complex is a combination of drift and diffusion. Note that in the special case $u = w$ the drift vanishes and the dynamics in l become purely diffusive.

As in Ref. [10], the average speed of unwinding is $v = \frac{1}{2}(u-w)$ or

$$v = \frac{1}{2}\sum_j (\alpha - \beta)P(j) + (s_{1f} + q_f - s_{1b} - r_b)P_1(j)$$

$$+ (s_{2f} + r_f - s_{2b} - q_b)P_2(j). \tag{24}$$

Similarly, the diffusion coefficient is $D = \frac{1}{4}(u+w)$, which is

$$D = \frac{1}{4}\sum_j (\alpha + \beta)P(j) + (s_{1f} + q_f + s_{1b} + r_b)P_1(j)$$

$$+ (s_{2f} + r_f + s_{2b} + q_b)P_2(j). \tag{25}$$

Note that if the sliding transitions represent unbiased diffusion, then the forward and backward rates $s_{\mu f}$ and $s_{\mu b}$ are equal. Then the terms involving the sliding rates drop out from the expression for v, but not from that for D.

V. SOLUTION

In order to evaluate the expressions for the unwinding velocity and diffusion coefficient, we must determine $P_1(j)$ and $P_2(j)$ in terms of the rate constants. Consider the result of summing Eqs. (14) and (15) over j to determine equations for the total probability of being in state 1, P_1, and the total probability of being in state 2, P_2. We can write these equations as

$$\frac{dP_1}{dt} = -k_{12}P_1 + k_{21}P_2, \qquad (26)$$

$$\frac{dP_2}{dt} = -k_{21}P_2 + k_{12}P_1, \qquad (27)$$

where the rate constant k_{12} depends on ω_{12}, q_f, and r_b and k_{21} depends on ω_{21}, r_f, and q_b. The steady-state solution has $P_2 = k_{12}/k_{21}P_1$.

This observation suggests a translationally invariant ratio of $P_1(j)$ and $P_2(j)$ when the rates are constant. We consider the case where the relative probability of being in state 1 or 2 is translationally invariant (independent of j). This must occur if the hopping rates are constant or spatially vary in the same way (for example, if states 1 and 2 have the same interaction potential with the dsNA). Since we are primarily interested in a passive helicase with constant rates, we will focus on this case. Because of the translational invariance, the probability in state 2 is a multiple of the probability in state 1, so that

$$P_2(j) = \gamma P_1(j). \qquad (28)$$

The zero-current relation requires that Eq. (16) equal zero, which requires

$$(\beta + s_{1f} + q_f)P_1(j+1) + (\beta + s_{2f} + r_f)P_2(j+1) = (\alpha + s_{1b} + r_b)P_1(j) + (\alpha + s_{2b} + q_b)P_2(j). \qquad (29)$$

We can plug Eq. (28) into Eq. (29) and solve for the unknown constant γ. We can rewrite Eq. (29) as a recursion relation that relates $P_1(j+1)$ to $P_1(j)$:

$$\frac{P_1(j+1)}{P_1(j)} = \frac{\alpha(1+\gamma) + s_{1b} + r_b + \gamma(s_{2b} + q_b)}{\beta(1+\gamma) + s_{1f} + q_f + \gamma(s_{2f} + r_f)} = c. \qquad (30)$$

Note that c is a function of γ. While it is possible to solve coupled equations for c and γ in general, the resulting expressions are long and not useful for developing intuition. Instead, we use the approximation relevant for helicases that α and β, the opening and closing rates of the NA, are several orders of magnitude larger than the other rates in the problem (see Ref. [10], where experimental data from Ref. [23] was used to estimate the opening rate $\alpha \sim 10^7$ s^{-1}; other rates in the problem are of order 10^2 s^{-1}). In this case, Eq. (30) reduces to

$$c \approx \frac{\alpha}{\beta}. \qquad (31)$$

Throughout the remainder of this paper, we will use this approximate value of c. Note that because α and β are con-

stant, c is also constant and Eq. (30) shows that $P_1(j)$ has power-law decay with increasing j (as in the BJ model for a passive helicase [10]).

Using Eqs. (28) and (30) in Eq. (14) at steady state and imposing the requirement that $P_1(j)$ cannot vanish for arbitrary j, we find a unique expression for γ:

$$\gamma = \frac{s_{1f}(1-c) - s_{1b}(c^{-1} - 1) + r_b + q_f + \omega_{12}}{cr_f + c^{-1}q_b + \omega_{21}}. \qquad (32)$$

With this result, we can evaluate Eqs. (24) and (25) and express v and D in a fashion analogous to the expressions in the simpler BJ model:

$$v = \frac{1}{2}\sum_j \mathcal{P}_1(j)(a + k^+ - b - k^-), \qquad (33)$$

$$D = \frac{1}{4}\sum_j \mathcal{P}_1(j)(a + k^+ + b + k^-), \qquad (34)$$

if we define the effective rates

$$a = \alpha(1+\gamma), \qquad (35)$$

$$b = \beta(1+\gamma), \qquad (36)$$

$$k^+ = \gamma(s_{2f} + r_f) + s_{1f} + q_f, \qquad (37)$$

$$k^- = \gamma(s_{2b} + q_b) + s_{1b} + r_b. \qquad (38)$$

Next we evaluate the sums in Eqs. (33) and (34), noting that $P_1(j) = P_1 c^j$ and taking into account that for $j=1$ the rates k^+ and b are zero. The result is

$$v = \frac{ck^+ - k^-}{2(1+\gamma)}, \qquad (39)$$

$$D = \frac{\alpha}{2} + \frac{ck^+ + k^-}{4(1+\gamma)}. \qquad (40)$$

Equations (39) and (40) are the main results.

Note that under most conditions the NA opening and closing rate α is orders of magnitude larger than the other rates, and therefore $D \approx \alpha/2$.

VI. COMPARISON WITH NS3 HELICASE

The NS3 helicase of the hepatitis C virus (HCV) is important for HCV replication and is therefore a potential drug target [24]. NS3 is also an interesting model helicase because it is the only currently known helicase capable of unwinding both dsRNA and dsDNA [25,26]. The flashing-ratchet mechanism proposed for NS3 helicase in Ref. [21] is a special case of the two-state model which we have developed in the preceding sections. In this section, we first briefly summarize the experimental data on NS3 helicase and their mutually contradictory interpretations which highlight the current debates in the literature. Then, we present analytical results for the special case of our model which captures the flashing-ratchet mechanism. We compare these theoretical

predictions with the corresponding experimental data for NS3 helicase. The comparisons are, however, limited by the contradictions between the observations in different experiments, many of which have been performed under different conditions.

A. Summary of experimental results on NS3 helicase

To compare our model to experiments on NS3 helicase, we would ideally like to know the enzyme's step size, the single-strand translocation rate, and the double-strand unwinding rate—including information on how it varies with NA sequence or applied force. Interpretation of experimental data on NS3 is complicated by differences in experiments done by different research groups. Some groups study the full-length NS3 protein, including the helicase and protease domains [27–31], while others study the helicase domain only [20,21,28,32–35]. Moreover, genetically different versions of NS3 can have different properties [36]. The NS3 protein can also function in different oligomeric states. In bulk solution experiments, full-length NS3 seems to function best as a dimer or higher-order oligomer [37], but single-molecule experiments can observe unwinding by NS3 monomers [30,31]. The helicase domain NS3h appears not to form dimers in solution [18,33,38], but multiple copies of the protein can bind to ssNA and unwind dsNA [33]. In at least one experiment, the kinetic parameters did not vary with the length of the ss tail used to load NS3h, suggesting that the helicase mechanism may not depend on whether the protein is a monomer or dimer [35].

Contradictory claims have been made in the literature on the qualitative description of NS3 helicase as well as on its quantitative characteristics. First, we consider the empirical evidence for the stepping pattern and the step size of NS3 helicase. Recently a detailed computational model of NS3, based on known crystal structures, supported the idea of single-base "inchworm" motion taken by NS3 monomers. This model of Zheng *et al.* proposes a major protein conformational change which is triggered by ATP binding and is coupled to forward motion of the helicase [39]. Models based on structural studies of NS3 have suggested single-base steps [18,40]. Similarly, structures of the distantly related Hel308 helicase, which shows some structural similarities to NS3, supports the idea of a ratchetlike mechanism during the ATP cycle [41]. However, most experimental efforts to determine the step size do not support single-base steps. Bulk kinetic experiments have given a kinetic step size of 9–17 base pairs, depending on protein form and unwinding substrate [27,29,35]. Single-molecule experiments on monomers of full-length NS3 have suggested a step size of 11 base pairs with 3 base-pair substeps [30] or 3 base pairs with 1 base-pair substeps [31]. The most recent single-molecule work has proposed that the fundamental step size is one base pair, with pauses occurring less frequently as part of the ssNA bound to the helicase occasionally "rips" off [31].

Next we summarize the current estimates of ss translocation rate and the speed of double-strand unwinding by NS3 helicase. The maximum ss translocation rate can be estimated from experiments that measure the ATP hydrolysis rate. In one experiment, the NS3h rate of ATP hydrolysis had a maximum k_{cat} of 80 s^{-1} in the presence of the single-stranded oligo dU$_{18}$ [32]. Assuming that during ss translocation the helicase hydrolyzes 1 ATP per step, this measurement sets an upper bound on the ss translocation velocity of 80 bases s^{-1}. The double-strand unwinding velocity of NS3 has been estimated from bulk and single-molecule experiments. In one single-turnover bulk kinetic study, the maximum unwinding rate of NS3h was 2.7 bp s^{-1} [35]; similar results were found by another group [28]. Full-length NS3 may unwind at higher velocities, up to 16.5 bp s^{-1} [27,28]. In single-molecule experiments with applied force, full-length NS3 monomers unwind at force-independent rates of 50 bp s^{-1} [30]. This relatively high velocity may be possible because of the applied force that reduces the energetic cost of opening the NA. In single-molecule FRET experiments on full-length NS3 monomers where no force is applied, an unwinding rate of $k \approx 0.9$ s^{-1} was measured for one base pair substeps [31]—a value closer to the bulk value measured for NS3h.

Finally, we examine the experimental data to investigate whether the unwinding by NS3 helicase is active or passive. The dependence of the unwinding rate on the base-pair binding free energy was measured both in single-molecule and bulk experiments. In the work of Dumont *et al.*, the RNA unwinding rate of full-length NS3 monomers was approximately independent of applied force in the range 9–17 pN [30]. In this experiment, the applied force was relatively high: the double strand melted at a force of 20 pN. In single-molecule experiments using a similar experimental setup, Cheng *et al.* [42] observed a significant effect of varying the RNA sequence on the NS3 unwinding rate. This observation of Cheng *et al.* indicates that a passive unwinding mechanism may not be adequate to explain the behavior of full-length NS3 helicase. Further, the apparent contradiction between the observations of Cheng *et al.* [42] and Dumont *et al.* [30] may be reconciled if we abandon the simple physical picture in which the base-pair binding free energy can be altered in a similar way by applied force or by changing the sequence. Recent bulk measurements examined the effects of sequence variation on the unwinding rate of NS3h [43]; this work is discussed below where we compare our theoretical predictions to experimental results.

In order to motivate our minimal model for the NS3 helicase, we now discuss the affinity of NS3h to NA and its modulation during the ATP hydrolysis cycle. Binding experiments on NS3h found that when the helicase is bound to an ATP analog, it binds to NA more weakly than when not bound to ATP or ADP [33,34]. The change in binding free energy is approximately 6 kT at room temperature (15 kJ mol^{-1}) [21]. In addition, the affinity of NS3h for ADP is low, so release of hydrolysis products is expected to be rapid [34]. These observations are the basis of the proposed flashing-ratchet mechanism of NS3h. (However, we note that another work has found no dependence of NA binding on the ATP hydrolysis state [28]; the source of this difference is unclear.)

B. Flashing-ratchet model of NS3 helicase

Here we consider a special case of our model which corresponds to a flashing-ratchet mechanism. Levin *et al.* pro-
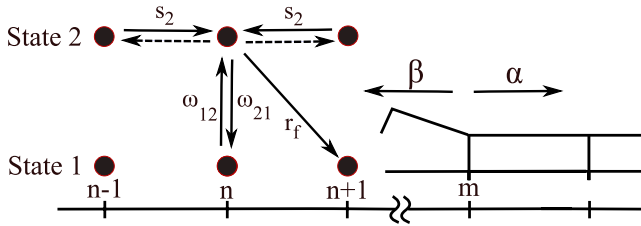
FIG. 2. (Color online) Schematic of the simplified model that represents a flashing ratchet. The protein can exist in either of two chemical states (labeled 1 and 2) at each lattice site (labeled n). Sliding transitions (where n changes, but the state does not) occur only in state 2 at rate s_2. Chemical transitions (where the state changes but n does not) occur at rates ω_{12} (for the transition from 1 to 2) and ω_{21} (for the transition from 2 to 1). A coupled transition (where both the state and n change) occurs at rate r_f (for the transition from 2 to 1 coupled to forward motion). The nucleic-acid single-strand–double-strand junction is at site m. The junction moves toward increasing m when the NA opens by one base (rate α) and toward decreasing m when the NA closes (rate β).

posed that NS3 helicase switches between two states: one tightly bound to the ssNA, the other weakly bound [20,21]. This scenario is referred to in the physics literature as a flashing ratchet [13]. When applying the flashing-ratchet scenario to NS3, the tightly bound state is represented by a periodic sawtooth potential (with periodicity of one ssNA base pair) and the weakly bound state is represented by a uniform (weakly position-independent) potential [21]. When comparing to the flashing-ratchet scenario, we will consider state 1 to represent the strongly bound (S) state and state 2 the weakly bound (W) state. By comparing the theoretical predictions for this special case of our model with the experimental data for NS3 helicase, we test whether or not NS3 follows the flashing-ratchet mechanism.

We assume that no sliding is possible in the tightly-bound state 1, so $s_{1f}=s_{1b}=0$, and that the sliding is unbiased in state 2, so $s_{2f}=s_{2b}=s_2$. To connect with the flashing-ratchet scenario and for simplicity, we assume that the rates $q_f=q_b=r_b=0$ (see Fig. 2). With these assumptions, we find that the rate of ss translocation is [from Eqs. (6) and (7)]

$$v_{ss} = \omega_{12} \frac{r_f}{r_f + \omega_{12} + \omega_{21}} \tag{41}$$

and the rate of ds unwinding is

$$v_u = \frac{\omega_{12}}{2} \frac{[c r_f - (1-c)s_2]}{c r_f + \omega_{12} + \omega_{21}}. \tag{42}$$

The excitation rate ω_{12} is associated with ATP binding and so is assumed proportional to ATP concentration. Therefore we write $\omega_{12}=\omega_0[\text{ATP}]$. The rates ω_{21} and r_f represent the relaxation from the weakly bound to the tightly bound state that occurs after ATP hydrolysis, product release, and diffusion in the weakly bound state. For a flashing ratchet, a high rate of forward motion will occur when the positions of the energy barriers and the time constants are such that forward movement (rate r_f) and return to the same place after one cycle (rate ω_{21}) occur with equal probability. To match this

optimal case, we therefore assume that $\omega_{21}=r_f$. Further, we assume that the sliding rate s_2 is small compared to the other rates; for concreteness, we will suppose $s_2=\epsilon r_f$ with $\epsilon=0.1$ unless otherwise stated. The velocities then become

$$v_{ss} = \frac{r_f \omega_0[\text{ATP}]}{\omega_0[\text{ATP}] + 2r_f}, \tag{43}$$

$$v_u = \frac{[c - \epsilon(1-c)]}{2} \frac{r_f \omega_0[\text{ATP}]}{\omega_0[\text{ATP}] + (1+c)r_f}. \tag{44}$$

Both v_{ss} and v_u are consistent with the Michaelis-Menten equation for enzyme kinetics, but with slightly different forms. Their ratio is

$$\frac{v_u}{v_{ss}} = \frac{[c - \epsilon(1-c)]}{2} \frac{\omega_0[\text{ATP}] + 2r_f}{\omega_0[\text{ATP}] + (1+c)r_f}. \tag{45}$$

In other words, we predict that the ratio of the unwinding velocity to the single-strand translocation velocity depends on ATP concentration. If we average over the sequence variation in DNA [9], we get the estimate $c=\alpha/\beta \approx 1/7$. For the purpose of quantitative illustration of the variation of $\frac{v_u}{v_{ss}}$ with ATP concentration, let us assume $\epsilon=1/10$. Then, $\frac{v_u}{v_{ss}} \approx 0.029$ at high ATP concentration and $\frac{v_u}{v_{ss}} \approx 0.05$ at low ATP concentration. This suggests that the ratio of the unwinding velocity to the single-strand translocation velocity could vary significantly with ATP concentration—the change is almost a factor of 2 for this example.

Next, we estimate v_u and v_{ss} for NS3 helicase. The single-strand translocation and unwinding velocities are fully determined by the parameters c, r_f, ω_0, ϵ, and ATP concentration; we now extract estimates of r_f and ω_0 from experimental data. In experiments at high ATP concentration and in the presence of ssNA, NS3h shows a maximum ATP hydrolysis rate of 80 s^{-1} [32]. If we take this value as the limiting ss-translocation rate and assume single base-pair steps, then $v_{ss}=80$ nt s^{-1} in the limit of high ATP concentration. Using this estimate of v_{ss} in Eq. (43), we get the estimate $r_f=80$ s^{-1}. This, in turn, implies that at high ATP concentration the unwinding velocity $v_u \approx 0.029 v_{ss} \approx 2.3$ bp s^{-1}. This value is comparable to the values of 2.7 bp s^{-1} [35] found for NS3h and 0.9 bp s^{-1} found for the 1-bp substeps of full-length NS3 [31]. We note that the unwinding velocity $v_u \ll v_{ss}$, as should be expected for this model which assumes a passive helicase mechanism. Experiments studying how NS3 ATPase activity [32] and unwinding [30] vary with ATP concentration found a similar Michaelis constant $K_m \approx 90$ μM. Using this value of K_m in Eq. (43), we estimate $\omega_0 = 2r_f/K_m \approx 1.8$ μM^{-1} s^{-1}.

The only remaining unknown parameter is $\epsilon=s_2/r_f$, the ratio of the sliding rate to the forward transition rate. A smaller value of ϵ means that the sliding transitions in the weakly bound state are less probable (see Fig. 2). A higher value of ϵ means that sliding transitions in the weakly bound state are more probable. This parameter has an important effect on the dependence of the helicase velocity on the base-pair binding free energy.
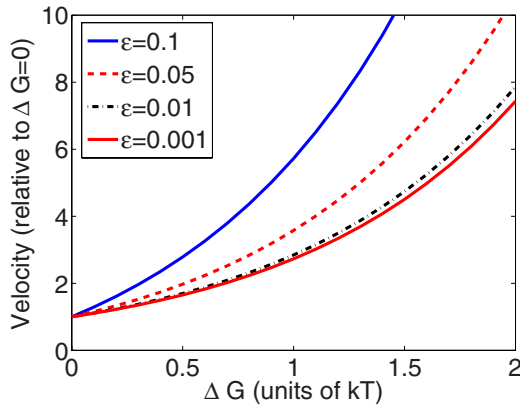
FIG. 3. (Color online) Dependence of the unwinding velocity on the base-pair binding free energy. The reference state is a value $c = 1/7$, which represents a sequence-averaged value for DNA. The additional destabilization energy ΔG (in units of kT) represents a free energy change that favors NA opening. When ϵ increases, the dependence of the velocity on ΔG becomes more pronounced. However, decreasing ϵ cannot flatten the curve indefinitely.

To study the effects of varying the base-pair binding free energy, we focus on the limit of high ATP concentration. In this case, if ΔG is the free energy of destabilization of base-pair binding, the parameter $c = \alpha/\beta$ varies according to $c = c_0 e^{\Delta G}$. Therefore, at high ATP concentration, the unwinding velocity varies as

$$\lim_{[\mathrm{ATP}]\to\infty} v_u = \frac{[c_0(1+\epsilon)e^{\Delta G} - \epsilon]}{2} r_f. \quad (46)$$

The unwinding velocity increases exponentially if the NA is destabilized, as one would expect for a passive helicase. However, the precise shape of the curve of unwinding velocity versus ΔG depends on ϵ. In the limit $\epsilon \to 0$, which physically means no helicase sliding transitions occur in the weakly bound state, the unwinding velocity varies with ΔG as a simple exponential:

$$\lim_{[\mathrm{ATP}]\to\infty,\epsilon\to 0} v_u = \frac{c_0 r_f}{2} e^{\Delta G}. \quad (47)$$

As ϵ increases, the helicase can slide in the weakly bound state. This allows more rapid unwinding by the helicase: when the dsNA is destabilized, the ds base just ahead of the helicase has an increased probability to be open. Rather than wait for the helicase chemical transitions to move forward, the helicase can take advantage of this increased junction open probability and slide forward. This allows the steeper rate of increase of v_u with ΔG seen in Fig. 3. This prediction is qualitatively consistent with the result of Tackett *et al.* [44], who found that full-length NS3 unwound double strands with higher melting temperatures less efficiently. However, in the single-molecule experiments of Dumont *et al.* the unwinding rate of full-length NS3 monomers was practically independent of applied force in the range 9–17 pN [30]. This disagrees with the prediction of this model if the only effect of the applied force is to change the binding free energy per base pair. However, this physical interpreta-

tion is clearly not valid, because recent experiments from the same laboratory find a significant variation in the RNA unwinding rate of full-length NS3 with the variation of the base composition of the RNA [42]. Reconciliation of the apparent contradictions in these experimental observations is possible by assuming an active helicase mechanism, which, however, is not incorporated in the current version of our model. Analyzing data from bulk experiments, Donmez *et al.* [43] claimed that the variation of NS3h unwinding velocity with base-pair binding free energy is inconsistent with a passive helicase mechanism. However, this conclusion is drawn from an analysis based on a reported single-strand translocation velocity of 6.4 bases s^{-1}, which is much lower than the value of 80 bases s^{-1} mentioned above. A ss translocation rate of 80 bases s^{-1} is an upper limit, assuming the helicase hydrolyzes 1 ATP per single-base step. If the helicase on average hydrolyzes >1 ATP per step, the ss translocation rate would be lower. A lower ss translocation rate would lead to an even larger disagreement between the passive helicase model we presented and the experimental data. We believe that a conclusive comparison between our model of a flashing-ratchet mechanism for NS3 helicase and the experimental data is not possible because of the contradictory reports of experimental studies.

VII. CONCLUSION

In this paper we have developed a general model of unwinding of a double-stranded nucleic acid molecule by a helicase motor. To capture some of the key features of the helicase mechanochemical cycle, we have modeled helicase switching between two chemical states. In this model, the sites of a discrete lattice represent the positions of the individual bases on the ssNA. At any spatial position, the helicase can exist in either of the two allowed chemical states. This model should be generally applicable to helicases where one of the transitions in the mechanochemical cycle is much slower than the other transitions. In this work, we have considered only a passive helicase mechanism—the helicase at the junction must wait for thermal fluctuations to open the dsNA before it can advance. In future work, it would be valuable to extend the model to include active destabilization of the dsNA by the helicase.

To compare the model in detail to experimental data, we focused on a special case which captures the flashing-ratchet mechanism proposed for the NS3 helicase [21]. Solving the master equations for this model at steady state, we have calculated the speed of unwinding and the speed of single-strand translocation. The ratio of the unwinding velocity to the ss translocation velocity varies with ATP concentration as well as with the base-pair binding free energy.

Our comparison to experimental data on NS3 helicase suggests that the model captures some features of the experiments. However, the experimental literature on NS3 contains contradictory results. This may be a result of the different genetic variants, protein truncations, oligomeric states, substrates, and buffer conditions used by different laboratories. A set of detailed experiments by different laboratories under consistent conditions may be important to fully understand the unwinding mechanism of NS3 helicase.

[1] B. Alberts, A. Johnson, J. Lewis, M. Raff, K. Roberts, and P. Walter, *Molecular Biology of the Cell*, 4th ed. (Garland, New York, 2002).

[2] *Molecular Motors*, edited by M. Schliwa (Wiley-VCH, Weinheim, 2003).

[3] C. Mavroidis, A. Dubey, and M. L. Yarmush, Annu. Rev. Biomed. Eng. **6**, 363 (2004).

[4] T. M. Lohman, K. Thorn, and R. D. Vale, Cell **93**, 9 (1998).

[5] J. Howard, *Mechanics of Motor Proteins and the Cytoskeleton* (Sinauer, Sunderland, MA, 2001).

[6] T. M. Lohman and K. P. Bjornson, Annu. Rev. Biochem. **65**, 169 (1996).

[7] E. Delagoutte and P. H. von Hippel, Q. Rev. Biophys. **35**, 431 (2002).

[8] S. S. Patel and K. M. Picha, Annu. Rev. Biochem. **69**, 651 (2000).

[9] M. D. Betterton and F. Jülicher, Phys. Rev. Lett. **91**, 258103 (2003).

[10] M. D. Betterton and F. Jülicher, J. Phys.: Condens. Matter **17**, S3851 (2005).

[11] M. D. Betterton and F. Jülicher, Phys. Rev. E **71**, 011904 (2005).

[12] We note that a two-state model for helicase translocation was also considered by Betterton and Jülicher [10], but the nature of the two states and the mechanism of translocation of the helicase are different from those developed here.

[13] F. Jülicher, A. Ajdari, and J. Prost, Rev. Mod. Phys. **69**, 1269 (1997).

[14] K. Nishinari, Y. Okada, A. Schadschneider, and D. Chowdhury, Phys. Rev. Lett. **95**, 118101 (2005).

[15] K. B. Zeldovich, J. F. Joanny, and J. Prost, Eur. Phys. J. E **17**, 155 (2005).

[16] Anatoly B. Kolomeisky and Michael E. Fisher, Annu. Rev. Phys. Chem. **58**, 675 (2007).

[17] K. P. Bjornson, I. Wong, and T. M. Lohman, J. Mol. Biol. **263**, 411 (1996).

[18] J. L. Kim, K. A. Morgenstern, J. P. Griffith, M. D. Dwyer, J. A. Thomson, M. A. Murcko, C. Lin, and P. R. Caron, Structure **6**, 89 (1998).

[19] S. S. Velankar, P. Soultanas, M. S. Dillingham, H. S. Subramanya, and D. B. Wigley, Cell **97**, 75 (1999).

[20] M. K. Levin, M. M. Gurjar, and S. S. Patel, J. Biol. Chem. **278**, 23311 (2003).

[21] M. K. Levin, M. Gurjar, and S. S. Patel, Nat. Struct. Mol. Biol. **12**, 429 (2005).

[22] Yariv Kafri, David K. Lubensky, and David R. Nelson, Biophys. J. **86**, 3373 (2004).

[23] G. Bonnet, O. Krichevsky, and A. Libchaber, Proc. Natl. Acad. Sci. U.S.A. **95**, 8602 (1998).

[24] D. N. Frick, Curr. Issues Mol. Biol. **9**, 1 (2007).

[25] D. W. Kim, Y. Gwack, J. H. Han, and J. Choe, Biochem. Biophys. Res. Commun. **215**, 160 (1995).

[26] C. L. Tai, W. K. Chi, D. S. Chen, and L. H. Hwang, J. Virol. **70**, 8477 (1996).

[27] V. Serebrov and A. M. Pyle, Nature (London) **430**, 476 (2004).

[28] N. David, J. Biol. Chem. **279**, 1269 (2004).

[29] R. K. F. Beran, M. M. Bruno, H. A. Bowers, E. Jankowsky, and A. M. Pyle, J. Mol. Biol. **358**, 974 (2006).

[30] S. Dumont, W. Cheng, V. Serebrov, R. K. Beran, I. Tinoco, A. M. Pyle, and C. Bustamante, Nature (London) **439**, 105 (2006).

[31] S. Myong, M. M. Bruno, A. M. Pyle, and T. Ha, Science **317**, 513 (2007).

[32] Frank Preugschat, Devron R. Averett, Berwyn E. Clarke, and David J. T. Porter, J. Biol. Chem. **271**, 24449 (1996).

[33] M. K. Levin and S. S. Patel, J. Biol. Chem. **274**, 31839 (1999).

[34] M. K. Levin and S. S. Patel, J. Biol. Chem. **277**, 29377 (2002).

[35] M. K. Levin, Y. H. Wang, and S. S. Patel, J. Biol. Chem. **279**, 26005 (2004).

[36] Angela M. I. Lamb, David Keeney, Patrick Q. Eckert, and David N. Frick, J. Virol. **77**, 3950 (2003).

[37] A. J. Tackett, Y. F. Chen, C. E. Cameron, and K. D. Raney, J. Biol. Chem. **280**, 10797 (2005).

[38] D. J. T. Porter, S. A. Short, M. H. Hanlon, F. Preugschat, J. E. Wilson, D. H. Willard, and T. G. Consler, J. Biol. Chem. **273**, 18906 (1998).

[39] W. J. Zheng, J. C. Liao, B. R. Brooks, and S. Doniach, Proteins: Struct., Funct., Bioinf. **67**, 886 (2007).

[40] N. H. Yao, T. Hesson, M. Cable, Z. Hong, A. D. Kwong, H. V. Le, and P. C. Weber, Nat. Struct. Biol. **4**, 463 (1997).

[41] K. Buttner, S. Nehring, and K. P. Hopfner, Nat. Struct. Mol. Biol. **14**, 647 (2007).

[42] Wei Cheng, Sophie Dumont, Jr., Ignacio Tinoco, and Carlos Bustamante, Proc. Natl. Acad. Sci. U.S.A. **104**, 13954 (2007).

[43] Ilker Donmez, Vaishnavi Rajagopal, Yong-Joo Jeong, and Smita S. Patel, J. Biol. Chem. **282**, 21116 (2007).

[44] A. J. Tackett, L. Wei, C. E. Cameron, and K. D. Raney, Nucleic Acids Res. **29**, 565 (2001).